Recipient-biased competition for a cross-fed nutrient is required for coexistence of microbial mutualists

Alexandra L. McCully, Breah LaSarre, James B. McKinlay[#]

Department of Biology, Indiana University, Bloomington, IN

Running title: Biased competition within a mutualism

[#]Corresponding author. 1001 E 3rd Street, Jordan Hall, Bloomington, IN 47405

Phone: 812-855-0359

Email: jmckinla@indiana.edu

Conflict of interest.

The authors declare no conflict of interest.

Abstract. Many mutualistic microbial relationships are based on nutrient cross-feeding. Traditionally, cross-feeding is viewed as being unidirectional from the producer to the recipient. This is likely true when a producer's metabolic waste, such as fermentation products, provides carbon for a recipient. However, in some cases the cross-fed nutrient holds value for both the producer and the recipient. In such cases, there is potential for nutrient reacquisition by producer cells in a population, leading to competition against recipients. Here we investigate the consequences of inter-partner competition for cross-fed nutrients on mutualism dynamics using an anaerobic coculture pairing fermentative *Escherichia coli* and phototrophic *Rhodopseudomonas palustris*. In this coculture, *E. coli* excretes waste organic acids that provide carbon for *R. palustris*. In return, *R. palustris* cross-feeds *E. coli* ammonium (NH_4^+), a valuable nitrogen compound that both species prefer. To explore the potential for inter-partner competition, we first used a kinetic model to simulate cocultures with varied affinities for NH_4^+ in each species. The model predicted that inter-partner competition for cross-fed NH_4^+ could profoundly impact population dynamics. We then experimentally tested the predictions by culturing mutants lacking NH_4^+ transporters in both NH_4^+ competition assays and cooperative cocultures. Both theoretical and experimental results indicated that the recipient must have a competitive advantage in acquiring valuable cross-fed NH_4^+ to avoid collapse of the mutualism. Thus, the very metabolites that form the basis for cooperative cross-feeding can also be subject to competition between mutualistic partners.

Significance. Mutualistic relationships, particularly those based on nutrient cross-feeding, promote stability of diverse ecosystems and drive global biogeochemical cycles. Cross-fed nutrients within these systems can be either waste products valued only by one partner or nutrients that both partners value. Here, we explore how inter-partner competition for a communally-valuable cross-fed nutrient impacts mutualism dynamics. We discovered that mutualism stability necessitates that the recipient have a competitive advantage against the producer in obtaining the cross-fed nutrient. We propose that the requirement for recipient-biased competition is a general rule for mutualistic coexistence based on the transfer of communally valuable resources, microbial or otherwise.

Introduction

Mutualistic cross-feeding of resources between microbes can have broad impacts ranging from influencing host health (1, 2) to driving global biogeochemical cycles (3–6). Cross-fed metabolites are often regarded as nutrients due to the value they provide to a dependent partner, the recipient. However, for the partner producing the nutrient, the producer, a cross-fed nutrient's value can vary. On one extreme, the cross-fed metabolite is valued by the recipient but not the producer, as is the case for fermentative waste products (7–10). In other cases, a cross-fed metabolite holds value for both the recipient and the producer, as is the case for vitamin B_{12} (6, 11, 12) and ammonium (NH_4^+) (13, 14). Such communally-valuable cross-fed nutrients are subject to partial privatization (15), wherein the producer has mechanisms to retain a portion of the nutrient pool for itself. While most mutualism cross-feeding studies only consider unidirectional metabolite transfer from producer to recipient, we wondered whether these mechanisms for partial privatization could lead to competition between partner populations for communally-valuable cross-fed nutrients. It seems likely that such competition could influence mutualism stability, as is known to be the case for competition for exogenous limiting resources (8, 16–19). To the best of our knowledge inter-partner competition for cross-fed nutrients and its impact on mutualism dynamics have never been investigated.

One example of cross-feeding that could involve competition between mutualistic partners is NH_4^+ excretion by N_2-fixing bacteria (Fig. 1A), called N_2-fixers (13, 14). During N_2 fixation, the enzyme nitrogenase converts N_2 gas into two NH_3 (20). In an aqueous environment, NH_3 is in equilibrium with NH_4^+. At neutral pH, NH_4^+ is the predominant form but small amounts of NH_3 can potentially leave the cell by diffusion across the membrane (21) (Fig. 1B). This inherent 'leakiness' for NH_3 likely fosters NH_4^+ cross-feeding, as extracellular NH_3 is available to neighboring microbes. Importantly, these neighbors can include clonal N_2-fixers, as NH_3/NH_4^+ is a preferred nitrogen source for most microbes. At concentrations above 20 μM, NH_3 can be acquired by passive diffusion; below 20 μM, NH_4^+ is bound and transported as NH_3 by AmtB transporters (Fig. 1B) (22). AmtB-like transporters are conserved throughout all domains of life (23). There is growing evidence that AmtB is used by N_2-fixers to recapture NH_3 lost

by passive diffusion, as ΔAmtB mutants accumulate NH_4^+ in culture supernatants whereas wild-type strains do not (24–26). Thus, during NH_4^+ cross-feeding, AmtB likely facilitates both NH_4^+ acquisition by the mutualistic partner and recapture of NH_4^+ by the N_2-fixer.

Assessing the effects of inter-partner competition for a cross-fed nutrient would require a level of experimental control not possible in most natural settings. However, synthetic microbial communities, or cocultures, are well-suited to address such questions (27–29). We previously developed a bacterial coculture that features cross-feeding of waste products (organic acids) from *Escherichia coli*, and a communally-valuable nutrient (NH_4^+) from *Rhodopseudomonas palustris* Nx (Fig. 1A) (26). Here, using both a kinetic model and genetic manipulation to alter the affinity of each species in the coculture for NH_4^+, we demonstrate that inter-partner competition for cross-fed NH_4^+ plays a direct role in maintaining coexistence. Specifically, insufficient competition by *E. coli* for NH_4^+ resulted in a collapse of the mutualism. Mutualism collapse could be delayed or potentially avoided through higher net NH_4^+ excretion by *R. palustris* or increased *E. coli* population size. Our results suggest that, as a general rule, competition for a cross-fed nutrient in an obligate mutualism must be biased in favor of the recipient to avoid mutualism collapse and the potential extinction of both species.

Results

Competition for cross-fed NH_4^+ is predicted to shape mutualism population dynamics. Within our coculture (Fig. 1A), *E. coli* (*Ec*) ferments sugars into waste organic acids, providing essential carbon and electrons to *R. palustris* (*Rp*) Nx. *R. palustris* Nx is genetically engineered to excrete low micromolar amounts of NH_4^+, providing essential nitrogen for *E. coli* (26). NH_4^+ excretion by *R. palustris* Nx is due to mutation of NifA, the master transcriptional regulator of nitrogenase, which results in constitutive nitrogenase activity even in the presence of normally inhibitory NH_4^+ (30). In contrast to organic acids, which are only useful to *R. palustris*, NH_4^+ produced by *R. palustris* Nx is essential for the growth of both species; *R. palustris* uses some NH_4^+ for its own biosynthesis and excretes the rest, which serves as the nitrogen source for *E. coli*. However, *R. palustris* Nx can also take up NH_4^+ (30). Thus, we hypothesized

that competition for cross-fed NH_4^+ between the *R. palustris* Nx producer population and the *E. coli* recipient population could influence mutualism dynamics.

We first explored whether competition for cross-fed NH_4^+ could affect the mutualism using SyFFoN, a mathematical model describing our coculture (26, 31). SyFFoN simulates population and metabolic dynamics in batch cocultures using Monod equations with experimentally-determined parameter values. As previous versions described NH_4^+ uptake kinetics only for *E. coli* (26, 31), we amended SyFFoN to include both an *R. palustris* NH_4^+ uptake affinity (K_m) and higher *R. palustris* maximum growth rate (μ_{MAX}) when NH_4^+ is used (SI Appendix Table S1). We then simulated batch cocultures wherein the relative affinity for NH_4^+ varied between the two species (Fig. 2). The model predicted that coexistence is maintained when the *R. palustris* affinity for NH_4^+ is low relative to that of *E. coli* (*Rp*:*Ec* < 1); sufficient N_2 is converted to NH_4^+ to support *R. palustris* growth and enough NH_4^+ is cross-fed to support *E. coli* growth. In contrast, when the *R. palustris* affinity for NH_4^+ is high relative to that of *E. coli* (*Rp*:*Ec* > 1), *E. coli* growth is no longer supported because *E. coli* cannot compete for excreted NH_4^+. However, high *R. palustris* cell densities were still predicted (Fig. 2) due to persistent, low-level organic acid cross-feeding stemming from *E. coli* maintenance metabolism, which can support *R. palustris* growth even when *E. coli* is not growing (31).

Genetic disruption of AmtB NH_4^+ transporters affects relative affinities for NH_4^+. Bacterial cells generally acquire NH_4^+ through two mechanisms: passive diffusion of NH_3, or active uptake by AmtB transporters (Fig. 1B). We hypothesized that deleting *amtB* genes in either species would result in a lower affinity for NH_4^+ in that species and thus could be used to test how relative NH_4^+ affinity impacts coculture dynamics. We generated ΔAmtB mutants of both *E. coli* and *R. palustris* and first characterized the effect of the mutations in monoculture. Deletion of *amtB* in *E. coli* had no effect on growth or fermentation profiles when NH_4Cl was in excess (SI Appendix Fig. S1), consistent with previous observations where ΔAmtB growth defects were only apparent at NH_4^+ concentrations below 20 μM (22). In *R. palustris* ΔAmtB monocultures with N_2 as the nitrogen source, growth trends were equivalent to

116 those of the parent strain; however, *R. palustris* ΔAmtB excreted more NH_4^+ than the parent strain and
117 about a third of that excreted by *R. palustris* Nx (SI Appendix Fig. S1C and D). In line with our
118 hypothesis, NH_4^+ excretion by *R. palustris* ΔAmtB could be due to a decreased ability to reacquire NH_4^+
119 lost by diffusion, resulting in increased net NH_4^+ excretion. Alternatively, we considered that NH_4^+
120 excretion by *R. palustris* ΔAmtB could be due to improper nitrogenase regulation. In several other N_2-
121 fixers, proper nitrogenase regulation requires AmtB, for example to induce post-translational nitrogenase
122 inhibition (switch-off) in response to NH_4^+ (25, 32). We tested whether *R. palustris* ΔAmtB exhibits
123 NH_4^+-induced switch-off by adding NH_4Cl to exponentially growing cultures and measuring H_2
124 production, an obligate product of the nitrogenase reaction (33), as a proxy for nitrogenase activity. Upon
125 adding NH_4Cl, H_2 production stopped in *R. palustris* ΔAmtB cultures. In contrast, H_2 production only
126 slowed slightly in *R. palustris* Nx cultures (SI Appendix Fig. S2), consistent with previous observations
127 for NifA* strains (34, 35). Additionally, like the parent strain, *R. palustris* ΔAmtB did not produce H_2
128 when grown with NH_4^+, unlike *R. palustris* Nx (SI Appendix Fig. S3). These observations demonstrate
129 that *R. palustris* ΔAmtB is competent for NH_4^+-induced nitrogenase repression, and thus NH_4^+ excretion
130 by *R. palustris* ΔAmtB is likely due to a poor ability to reacquire NH_4^+ lost by diffusion.
131 To test our hypothesis that deleting *amtB* would lower cellular affinity for NH_4^+, we directly
132 competed all possible *E. coli* and *R. palustris* strain combinations in competition assays where ample
133 carbon was available for each species but the NH_4^+ concentration was kept low; specifically, a small
134 amount of NH_4^+ was added every hour to bring the final NH_4^+ concentration to 5 μM (Fig. 3). In this
135 competition assay, the species that is more competitive for NH_4^+ should reach a higher cell density than
136 the other species. In all cases, WT *E. coli* was more competitive for NH_4^+ than *R. palustris*. However,
137 each *R. palustris* strain was able to outcompete *E. coli* ΔAmtB (Fig. 3), even though the *R. palustris*
138 maximum growth rate is 4.6-times slower than that of *E. coli* (SI Appendix Fig. S1). Even *R. palustris*
139 strains lacking AmtB outcompeted *E. coli* ΔAmtB (Fig. 3), indicating that *R. palustris* has a higher
140 affinity for NH_4^+ than *E. coli* independent of AmtB. These data confirmed that deletion of *amtB* was an
141 effective means by which to lower the relative affinity for NH_4^+ in each mutualistic partner.

Altering relative NH_4^+ affinities affects mutualistic partner frequencies. We then examined how relative affinities for NH_4^+ influenced mutualism dynamics by comparing the growth trends of cocultures containing either WT *E. coli* or *E. coli* ΔAmtB, paired with either *R. palustris* ΔAmtB, *R. palustris* Nx, or *R. palustris* NxΔAmtB, the latter of which we previously determined to exhibit 3-fold higher NH_4^+-excretion levels than the Nx strain in monoculture (26). For each *R. palustris* partner, cocultures with *E. coli* ΔAmtB grew slower than cocultures with WT *E. coli* (Fig. 4A,B). *E. coli* ΔAmtB also constituted a lower percentage of the population and achieved lower cell densities compared to WT *E. coli* when paired with the same *R. palustris* strain (Fig. 4C). These lower frequencies were consistent with the competitive disadvantage of *E. coli* ΔAmtB for excreted NH_4^+ (Fig. 3).

For *R. palustris* strains lacking AmtB, the effects on population trends varied. Consistent with our previous work, *R. palustris* NxΔAmtB supported higher WT *E. coli* percentages and cell densities (Fig. 4C) (26). With high NH_4^+ excretion levels from *R. palustris* NxΔAmtB, faster *E. coli* growth leads to rapid organic acid accumulation, which acidifies the environment, inhibits *R. palustris* growth, and leaves organic acids unconsumed (Fig. 4D) (26). Surprisingly, although *R. palustris* ΔAmtB excreted less NH_4^+ than *R. palustris* Nx in monoculture, *R. palustris* ΔAmtB supported a higher WT *E. coli* population in coculture and consumable organic acids accumulated (Fig. 4C, D). These trends resemble those from cocultures with *R. palustris* NxΔAmtB (Fig. 4C, D), which has a high level of NH_4^+ excretion (SI Appendix Fig. S1D). Unlike Nx strains, which have constitutive nitrogenase activity due to a mutation in the transcriptional activator NifA (30), *R. palustris* ΔAmtB has WT NifA. Thus, *R. palustris* ΔAmtB can likely still regulate nitrogenase expression, and thereby its activity, in response to nitrogen starvation. We hypothesized that in coculture with WT *E. coli*, *R. palustris* ΔAmtB might experience heightened nitrogen starvation, as NH_4^+ consumption by WT *E. coli* would limit NH_4^+ reacquisition by *R. palustris* ΔAmtB (in an *R. palustris* ΔAmtB monoculture any lost NH_4^+ would remain available to *R. palustris*). We therefore tested whether coculture conditions stimulated higher nitrogenase activity using an acetylene reduction assay. In agreement with our hypothesis, *R. palustris* ΔAmtB had increased nitrogenase activity in coculture conditions compared to monocultures, whereas *R. palustris* Nx, which

exhibits constitutive nitrogenase activity, showed similar levels in both conditions (SI Appendix Fig. S4). Thus, the relatively high WT *E. coli* population in coculture with *R. palustris* ΔAmtB is likely due to both the competitive advantage for acquiring NH_4^+ over *R. palustris* ΔAmtB (Fig. 3) and higher NH_4^+ cross-feeding levels due to increased nitrogenase activity.

***E. coli* must have a competitive advantage for NH_4^+ acquisition to avoid mutualism collapse.** We were surprised to observe that cocultures of *R. palustris* ΔAmtB paired with *E. coli* ΔAmtB showed little growth when started from a single colony of each species (Fig. 4A), a method that we routinely use to initiate cocultures (26, 31). We reasoned that the higher *R. palustris* ΔAmtB affinity for NH_4^+ relative to *E. coli* ΔAmtB (Fig. 3) likely led to community collapse as predicted by SyFFoN (Fig. 2). Even though SyFFoN had predicted *R. palustris* growth when outcompeting *E. coli* for NH_4^+ (Fig. 2), SyFFoN likely underestimates the time required to achieve these densities, if they would be achieved at all, as SyFFoN does not take into account cell death, which is known to occur when *E. coli* growth is prevented (31). Consistent with the hypothesis that poor coculture growth was due to a competitive disadvantage of *E. coli* ΔAmtB for NH_4^+, SyFFoN simulations indicated that starting with a larger *E. coli* ΔAmtB population would increase the probability that any given *E. coli* cell would acquire NH_4^+ versus *R. palustris* and thereby overcome the competitive disadvantage of *E. coli* ΔAmtB for NH_4^+ (SI Appendix Fig. S5). Indeed, we observed greater growth of both species when cocultures were inoculated with equal or higher relative densities of *E. coli* ΔAmtB versus *R. palustris* ΔAmtB (SI Appendix Fig. S5).

The explanation that mutualism collapse was due to a competitive advantage of *R. palustris* ΔAmtB over *E. coli* ΔAmtB for NH_4^+ called into question why cocultures pairing *E. coli* ΔAmtB with either *R. palustris* Nx or *R. palustris* NxΔAmtB did not collapse as well (Fig. 4), given that in all of these pairings *E. coli* ΔAmtB is at competitive disadvantage (Fig. 3). We hypothesized that a relatively high NH_4^+ excretion level by these latter *R. palustris* strains (SI Appendix Fig. S1D) could compensate for a low *E. coli* NH_4^+ affinity. To explore this hypothesis we simulated cocultures with the *R. palustris* affinity for NH_4^+ set high relative to that of *E. coli* (*Rp*:*Ec* = 1000) and varied the *R. palustris* NH_4^+ excretion level

(Fig. 5). Indeed, increasing *R. palustris* NH_4^+ excretion was predicted to overcome a low *E. coli* affinity for NH_4^+ and support growth of both species (Fig. 5). The only exception was at the highest levels of NH_4^+ excretion, where *R. palustris* growth was predicted to be inhibited due to rapid *E. coli* growth and subsequent accumulation of organic acids that acidify the environment (Fig. 5) (26). These simulations suggested that *R. palustris* Nx and NxΔAmtB supported coculture growth with *E. coli* ΔAmtB due to higher NH_4^+ excretion levels (SI Appendix Fig. S1D), whereas a combination of low NH_4^+ excretion by *R. palustris* ΔAmtB (SI Appendix Fig. S1D) and a low affinity for NH_4^+ by *E. coli* ΔAmtB led to collapse of the mutualism in this pairing.

So far, we had only considered the effect of severe discrepancies in NH_4^+ affinities between the two species (e.g., 1000-fold difference in K_m values in our simulations) as a mechanism leading to coculture collapse within the time period of a single culturing. However, we wondered if a subtle discrepancy in NH_4^+ affinities could lead to coculture collapse if given more time. We therefore simulated serial transfers of cocultures with partners having different relative NH_4^+ affinities (Fig. 6A, B). At equivalent NH_4^+ affinities (Fig. 6A), both species were predicted to be maintained over serial transfers. However, when the relative affinities approached a threshold (relative *Rp*:*Ec* = 2.75), cell densities of both species were predicted to decrease over serial transfers (Fig. 6B). This decline in coculture growth is due to *E. coli* being slowly but progressively outcompeted for NH_4^+ by *R. palustris*. As the difference between the *R. palustris* and *E. coli* populations expands, *R. palustris* cells have a greater chance of acquiring NH_4^+ than the smaller *E. coli* population, further starving *E. coli* and simultaneously cutting off *R. palustris* from its supply of organic acids from *E. coli.*

The above prediction prompted us to investigate if cocultures pairing *R. palustris* Nx with *E. coli* ΔAmtB were stable through serial transfers. We focused on cocultures with *R. palustris* Nx rather than *R. palustris* NxΔAmtB because *R. palustris* Nx has AmtB and would therefore be most likely to outcompete *E. coli* ΔAmtB. Strikingly, after eight serial transfers of cocultures pairing *R. palustris* Nx with *E. coli* ΔAmtB we observed coculture collapse (Fig. 6C). This observation is in stark contrast to cocultures of *R. palustris* Nx paired with WT *E. coli*, which we have serially transferred for over 100 times with no

extinction events (unpublished data). These results indicate that the recipient population must have a competitive advantage for a cross-fed nutrient versus the producer population to avoid mutualism collapse.

Discussion

Here we demonstrate that mutualistic partners can compete for a cross-fed nutrient upon which the mutualistic interaction is based, in this case NH_4^+. This competition can impact partner frequencies and mutualism stability. Efficient nutrient reacquisition by the producer can render nutrient excretion levels insufficient for cooperative growth, starving the recipient and leading to tragedy of the commons (36). Conversely, recipient-biased competition for a cross-fed nutrient drives cooperative directionality in nutrient exchange and thereby promotes mutualism stability. One implication of these results is that inter-partner competition can influence the level of resource privatization. Within microbial interdependencies, partial privatization has primarily been thought to depend on mechanisms used by the producer to retain a portion of a communally-valuable resource (15). Our data indicate that for excreted resources having a transient availability to both mutualists, recipient acquisition mechanisms can also influence the level of producer privatization, as the competition impacts how much of a cross-fed resource will be shared versus re-acquired. In effect, recipient-biased competition avoids tragedy of the commons by enforcing partial privatization of a communally-valuable resource. The importance of the recipient having the upper hand in inter-partner competition likely applies to other synthetic cocultures and natural microbial mutualisms that are based on the cross-feeding of communally-valuable nutrients, including amino acids (37, 38) and vitamin B_{12} (6, 11). The same rule could also apply to inter-kingdom and non-microbial examples of cross-feeding (e.g., plants and pollinators, nutrient transfer between plants and bacteria or fungi (39)) and cooperative feeding (e.g., honeyguide bird and human harvesting of bee hives (40), cooperative hunting between grouper fish and moray eels (41)). In such cases, increased privatization of a cross-fed or shared resource, for example through producer-biased competition, could threaten the mutualism upon which both species depend (15, 39, 42).

In our system, AmtB transporters were crucial determinants of inter-partner competition for NH_4^+. We were intrigued to find that when both species lacked AmtB, *R. palustris* out-competed *E. coli* for NH_4^+ (Fig. 5), enough so to collapse the mutualism within a single culturing (Fig. 3). Whether by maximizing NH_4^+ retention or re-acquisition, *R. palustris*, and perhaps other N_2-fixers, might have additional mechanisms aside from AmtB to minimize loss of NH_4^+ as NH_3. These mechanisms could include a relatively low internal pH to favor NH_4^+ over NH_3, negatively-charged surface features, or relatively high affinities by NH_4^+-assimilating enzymes such as glutamine synthetase. There are several reasons why it would be beneficial for N_2-fixers to minimize NH_4^+ loss. First, N_2 fixation is expensive, both in terms of the enzymes involved (43) and the reaction itself, costing 16 ATP to convert one N_2 into two NH_3 (33). Passive loss of NH_3 would only add to this cost, as more N_2 would have to be fixed to compensate. Second, loss of NH_4^+ could benefit nearby microbes competing against an N_2-fixer for separate limiting nutrients (14, 44). The possibility that N_2-fixers could have a superior ability to retain or acquire NH_4^+ independently of AmtB is not farfetched. Bacteria are known to exhibit differential abilities to compete for nutrients. For example, iron acquisition commonly involves iron-binding siderophores, but siderophores can be chemically distinct and thereby differ in their affinity for iron (45). Strategies to utilize siderophores as a shared resource are also numerous, leading to different cooperative or competitive outcomes in microbial communities (45, 46). One must consider that additional mechanisms for acquiring NH_4^+ beyond AmtB might likewise exist. As our results have raised the potential for inter-partner competition for cross-fed resources themselves, understanding the physiological mechanisms that confer competitive advantages for nutrient acquisition between species will undoubtedly aid in describing the interplay between competition and cooperation within mutualisms.

Materials and Methods

Strains and growth conditions. Strains, plasmids, and primers are listed in SI Appendix Table S2. All *R. palustris* strains contained *ΔuppE* and *ΔhupS* mutations to facilitate accurate colony forming unit (CFU) measurements by preventing cell aggregation (47) and to prevent H_2 uptake, respectively. *E. coli* was

cultivated on Luria-Burtani (LB) agar and *R. palustris* on defined mineral (PM) (48) agar with 10 mM succinate. $(NH_4)_2SO_4$ was omitted from PM agar for determining *R. palustris* CFUs. Monocultures and cocultures were grown in 10-mL of defined M9-derived coculture medium (MDC) (26) in 27-mL anaerobic test tubes. To make the medium anaerobic, MDC was bubbled with N_2, then tubes were sealed with rubber stoppers and aluminum crimps, and then autoclaved. After autoclaving, MDC was supplemented with cation solution (1 % v/v; 100 mM $MgSO_4$ and 10 mM $CaCl_2$) and glucose (25 mM), unless indicated otherwise. *E. coli* monocultures were also supplemented with 15mM NH_4Cl. All cultures were grown at 30°C laying horizontally under a 60 W incandescent bulb with shaking at 150 rpm. Starter cocultures were inoculated with 200 µL MDC containing a suspension of a single colony of each species. Test cocultures were inoculated using a 1% inoculum from starter cocultures. Serial transfers were also inoculated with a 1% inoculum. Kanamycin and gentamycin were added to a final concentration of 100 µg/ml for *R. palustris* and 15 µg/ml for *E. coli* where appropriate.

Generation of *R. palustris* mutants. *R. palustris* mutants were derived from wild-type CGA009 (49). Generation of strains CGA4004, CGA4005, and CGA4021 was described previously (26). For generation of strain CGA4026 (*R. palustris* ΔAmtB) the WT *nifA* gene was amplified using primers JBM1 and JBM2, digested with XbaI and BamHI, and ligated into plasmid pJQ200SK to make pJQnifA16. This suicide vector was then introduced into CGA4021 by conjugation, and sequential selection and screening was performed as described (50) to replace *nifA** with WT *nifA*. Reintroduction of the WT *nifA* gene was confirmed by PCR and sequencing.

Generation of the *E. coli* ΔAmtB mutant. P1 transduction (51) was used to introduce Δ*amtB::Km* from the Keio collection strain JW0441-1 (52) into MG1655. The Δ*amtB::Km* genotype of kanamycin-resistant colonies was confirmed by PCR and sequencing.

Analytical procedures. Cell density was assayed by optical density at 660 nm (OD_{660}) using a Genesys 20 visible spectrophotometer (Thermo-Fisher, Waltham, MA, USA). Growth curve readings were taken in culture tubes without sampling (i.e., Tube OD_{660}). Specific growth rates were determined using readings between 0.1-1.0 OD_{660} where there is linear correlation between cell density and OD_{660}. Final

298 OD_{660} measurements were taken in cuvettes and samples were diluted into the linear range as necessary.
299 H_2 was quantified using a Shimadzu (Kyoto, Japan) gas chromatograph (GC) with a thermal conductivity
300 detector as described (53). Glucose, organic acids, formate and ethanol were quantified using a Shimadzu
301 high-performance liquid chromatograph (HPLC) as described (54). NH_4^+ was quantified using an
302 indophenol colorimetric assay as described (26).
303 **Nitrogenase activity.** Nitrogenase activity was measured using an acetylene reduction assay (43). Cells
304 from 10-mL cultures were harvested and resuspended in 10-mL fresh MDC medium in 27-mL sealed
305 tubes pre-flushed with argon gas. Suspensions were incubated in light for 1 h at 30°C to recover. Then,
306 250 µl of 100% acetylene gas was injected into the headspace to initiate the assay, and ethylene
307 production was measured over time by gas chromatography as described (43). Ethylene levels were
308 normalized to total *R. palustris* CFUs in the 10-ml volume.
309 **NH_4^+ competition assay.** Fed-batch cultures were performed in custom anaerobic 75-ml serum vials with
310 side sampling ports. Each vial contained a stir bar and 30-mL of MDC, and was sealed at both ends with
311 rubber stoppers and aluminum crimps. Each vial was supplemented with 25 mM glucose, 1 % v/v cation
312 solution and 20 mM sodium acetate. Starter monocultures of each species were grown to equivalent
313 CFUs/mL in MDC tubes containing limiting nutrients (3 mM sodium acetate for *R. palustris* and 1.5 mM
314 NH_4Cl for *E. coli*), and 1 mL of each species was inoculated into the serum vials. These competition
315 cocultures were incubated at 30°C under a 60 W incandescent bulb with stirring at 200 rpm (Thermo
316 Scientific) for 96 h. Each serum vial was constantly flushed with Ar to maintain anaerobic conditions.
317 NH_4Cl was fed from a 500 µM NH_4Cl stock using a peristaltic pump (Watson-Marlow) on an automatic
318 timer (Intermatic DT620) at a rate of 0.33 mL/min once an hour for a final concentration of ~ 5 µM upon
319 each addition. Samples were taken at 0 and 96 h for quantification of CFUs.
320 **Mathematical modeling.** A Monod model describing bi-directional cross-feeding in batch cultures,
321 called SyFFoN_v3 (Syntrophy between Fermenter and Fixer of Nitrogen), was modified from our
322 previous model (31) to allow for competition between *E. coli* and *R. palustris* for NH_4^+ as follows: (i) an
323 equation for *R. palustris* growth rate on NH_4^+ was added to boost the *R. palustris* growth rate when

acquiring NH_4^+ and (ii) the ability for *R. palustris* to consume NH_4^+ was added along with a K_m of *R. palustris* for NH_4^+ (K_{AR}). Equations and default parameter values are in the SI Appendix and Table S1. SyFFoN_v3 runs in R studio and is available for download at: https://github.com/McKinlab/Coculture-Mutualism.

Acknowledgments

We thank Richard Phillips (Indiana University) for providing equipment for the NH_4^+ competition assay. We also thank Jay Lennon (Indiana University) for helpful discussions on the manuscript. This work was supported in part by the U.S. Department of Energy, Office of Science, Office of Biological and Environmental Research, under Award Number DE-SC0008131, by the U.S. Army Research Office, grant W911NF-14-1-0411, and by the Indiana University College of Arts and Sciences.

References

1. Flint HJ, Duncan SH, Scott KP, Louis P. (2007) Interactions and competition within the microbial community of the human colon: Links between diet and health. *Environ Microbiol.* **9**(5):1101–1111.
2. Hammer ND, et al. (2014) Inter- and intraspecies metabolite exchange promotes virulence of antibiotic-resistant *Staphylococcus aureus*. *Cell Host Microbe.* **16**(4):531–537.
3. McInerney MJ, Sieber JR, Gunsalus RP. (2010) Syntrophy in anaerobic global carbon cycles. *Curr Opin Biotechnol.* **20**(6):623–632.
4. Durham BP, et al. (2015) Cryptic carbon and sulfur cycling between surface ocean plankton. *Proc Natl Acad Sci U S A.* **112**(2):453–457.
5. Reeburgh WS. (2007) Oceanic Methane Biogeochemistry. *Chem Rev.* **107**(2):486–513.
6. Croft MT, Lawrence AD, Raux-Deery E, Warren MJ, Smith AG. (2005) Algae acquire vitamin B_{12} through a symbiotic relationship with bacteria. *Nature.* **438**:90–93.
7. McInerney MJ, et al. (2008) Physiology, ecology, phylogeny, and genomics of microorganisms capable of syntrophic metabolism. *Ann N Y Acad Sci.* **1125**:58–72.

8. Hillesland KL, Stahl DA. (2010) Rapid evolution of stability and productivity at the origin of a microbial mutualism. *Proc Natl Acad Sci U S A.* **107**(5):2124–2129.
9. Schink B. (1997) Energetics of syntrophic cooperation in methanogenic degradation. *Microbiol Mol Biol Rev.* **61**(2):262–280.
10. Stams AJM. (1994) Metabolic interactions between anaerobic bacteria in methanogenic environments. *Antonie van Leeuwenhoek, Int J Gen Mol Microbiol.* **66**:271–294.
11. Grant MA, Kazamia E, Cicuta P, Smith AG. (2014) Direct exchange of vitamin B_{12} is demonstrated by modeling the growth dynamics of algal-bacterial cocultures. *ISME J* **8**(7):1–10.
12. Seth EC, Taga ME. (2014) Nutrient cross-feeding in the microbial world. *Front Microbiol.* **5**:1-6.
13. Behrens S, et al. (2008) Linking microbial phylogeny to metabolic activity at the single-cell level by using enhanced element labeling-catalyzed reporter deposition fluorescence in situ hybridization (EL-FISH) and NanoSIMS. *Appl Environ Microbiol.* **74**(10):3143–3150.
14. Adam B et al. (2016) N_2-fixation, ammonium release and N-transfer to the microbial and classical food web within a plankton community. *ISME J.* **10**:450-459.
15. Estrela S, Morris JJ, Kerr B (2016) Private benefits and metabolic conflicts shape the emergence of microbial interdependencies. *Environ Microbiol.* **18**(5):1415–1427.
16. Meyer JS, Tsuchiya HM. (1975) Dynamics of mixed populations having complementary metabolism. *Biotechnol Bioeng.* **17**:1065–1081.
17. Kim HJ, Boedicker JQ, Choi JW, Ismagilov RF. (2008) Defined spatial structure stabilizes a synthetic multispecies bacterial community. *Proc Natl Acad Sci U S A.* **105**(47):18188–18193.
18. Miura Y, Tanaka H, Okazaki M. (1980) Stability analysis of commensal and mutual relations with competitive assimilation in continuous mixed culture. *Biotechnol Bioeng.* **22**(5):929–946.
19. Estrela S, Trisos CH, Brown SP. (2012) From metabolism to ecology: cross-feeding interactions shape the balance between polymicrobial conflict and mutualism. *Am Nat.* **180**(5):566–576.
20. Bulen WA, LeComte JR. (1966) The nitrogenase system from *Azotobacter*: two-enzyme requirement for N_2 reduction, ATP-dependent H_2 evolution, and ATP hydrolysis. *Proc Natl Acad Sci U S A.* **56**(3):979–986.

21. Walter A, Gutknecht J. (1986) Permeability of small nonelectrolytes through lipid bilayer membranes. *J Membr Biol.* **90**(3):207–217.

22. Kim M, et al. (2012) Need-based activation of ammonium uptake in *Escherichia coli*. *Mol Syst Biol* **8**(616):1–10.

23. Peng J, Huang CH. (2006) Rh proteins vs Amt proteins: an organismal and phylogenetic perspective on CO_2 and NH_3 gas channels. *Transfus Clin Biol.* **13**(1–2):85–94.

24. Barney BM, Eberhart LJ, Ohlert JM, Knutson CM, Plunkett MH. (2015) Gene deletions resulting in increased nitrogen release by *Azotobacter vinelandii*: Application of a novel nitrogen biosensor. *Appl Environ Microbiol.* **81**(13):4316–4328.

25. Zhang T, et al. (2012) Involvement of the ammonium transporter AmtB in nitrogenase regulation and ammonium excretion in *Pseudomonas stutzeri* A1501. *Res Microbiol.* **163**(5):332–339.

26. LaSarre B, McCully AL, Lennon JT, McKinlay JB. (2017) Microbial mutualism dynamics governed by dose-dependent toxicity of cross-fed nutrients. *ISME J*. **11**:337–348.

27. Widder S, et al. (2016) Challenges in microbial ecology: building predictive understanding of community function and dynamics. *ISME J.* **10**:2557–2568.

28. Momeni B, Chen CC, Hillesland KL, Waite A, Shou W. (2011) Using artificial systems to explore the ecology and evolution of symbioses. *Cell Mol Life Sci.* **68**(8):1353–1368.

29. Lindemann SR, et al. (2016) Engineering microbial consortia for controllable outputs. *ISME J.* **10**:2077–2084.

30. McKinlay JB, Harwood CS. (2010) Carbon dioxide fixation as a central redox cofactor recycling mechanism in bacteria. *Proc Natl Acad Sci U S A*. **107**(26):11669–11675.

31. McCully AL, LaSarre B, McKinlay JB. (2017) Growth-independent cross-feeding modifies boundaries for coexistence in a bacterial mutualism. *biorXiv*. **doi:** https://doi.org/10.1101/083386

32. Yakunin AF, Hallenbeck PC. (2002) AmtB is necessary for NH_4^+-induced nitrogenase switch-off and ADP-ribosylation in *Rhodobacter capsulatus*. *J Bacteriol.* **184**(15):4081–4088.

33. Hoffman BM, Lukoyanov D, Dean DR, Seefeldt LC. (2013) Nitrogenase: A draft mechanism. *Acc Chem Res*. **46**(2):587–595.

34. Rey FE, Heiniger EK, Harwood CS. (2007) Redirection of metabolism for biological hydrogen production. *Appl Environ Microbiol.* **73**(5):1665–1671.

35. Heiniger EK, Oda Y, Samanta SK, Harwood CS. (2012) How posttranslational modification of nitrogenase is circumvented in *Rhodopseudomonas palustris* strains that produce hydrogen gas constitutively. *Appl Environ Microbiol.* **78**(4):1023–1032.

36. Rankin DJ, Bargum K, Kokko H. (2007) The tragedy of the commons in evolutionary biology. *Trends Ecol Evol.* **22**(12):643–651.

37. Pande S, et al. (2014) Fitness and stability of obligate cross-feeding interactions that emerge upon gene loss in bacteria. *ISME J.* **8**(5):953–62.

38. Harcombe W. (2010) Novel cooperation experimentally evolved between species. *Evolution.* **64**(7):2166–2172.

39. Bronstein JL. (2001) The Exploitation of Mutualisms. *Ecol Lett.* **4**:277–287.

40. Isack HA, Reyer H-U. (1989) Honeyguides and honey gatherers: Interspecific communication in a symbiotic relationship. *Science.* **243**(4896):1343–1346.

41. Bshary R, Hohner A, Ait-el-Djoudi K, Fricke H. (2006) Interspecific communicative and coordinated hunting between groupers and giant moray eels in the red sea. *PLoS Biol* **4**(12):2393–2398.

42. Sachs JL, Mueller UG, Wilcox TP, Bull JJ. (2004) The evolution of cooperation. *Q Rev Biol.* **51**(2):211–244.

43. Oda Y, et al. (2005) Functional genomic analysis of three nitrogenase isozymes in the photosynthetic bacterium *Rhodopseudomonas palustris*. *Am Soc Microbiol.* 187(22):7784–7794.

44. Morris JJ, Lenski RE, Zinser ER. (2012) The black queen hypothesis: Evolution of dependencies through adaptive gene loss. *mBio.* **3**(2):1–7.

45. Joshi F, Archana G, Desai A. (2006) Siderophore cross-utilization amongst rhizospheric bacteria and the role of their differential affinities for Fe^{3+} on growth stimulation under iron-limited conditions. *Curr Microbiol.* **53**(2):141–147.

46. Niehus R, Picot A, Oliveira NM, Mitri S, Foster KR. (2017) The evolution of siderophore production as a competitive trait. *Evolution*. doi:10.1111/evo.13230.

431 47. Fritts RK, Lasarre B, Stoner AM, Posto AL, Mckinlay JB (2017) A *Rhizobiales*-specific unipolar
432 polysaccharide adhesin contributes to *Rhodopseudomonas palustris* biofilm formation across diverse
433 photoheterotrophic conditions. *Appl Environ Microbiol.* **83**(4):1–14.
434 48. Kim M-K, Harwood CS (1991) Regulation of benzoate-CoA ligase in *Rhodopseudomonas palustris*.
435 *FEMS Microbiol Lett.* **83**:199–203.
436 49. Larimer FW, et al. (2004) Complete genome sequence of the metabolically versatile photosynthetic
437 bacterium *Rhodopseudomonas palustris*. *Nat Biotechnol.* **22**(1):55–61.
438 50. Rey FE, Oda Y, Harwood CS. (2006) Regulation of uptake hydrogenase and effects of hydrogen
439 utilization on gene expression in *Rhodopseudomonas palustris*. *J Bacteriol.* **188**(17):6143–6152.
440 51. Thomason LC, Costantino N, Court DL. (2007) *E. coli* Genome manipulation by P1 transduction. *Curr*
441 *Protoc Mol Biol.* doi 10.1002/0471142727.mb0117s79
442 52. Baba T, et al. (2006) Construction of *Escherichia coli* K-12 in-frame, single-gene knockout mutants: the
443 Keio collection. *Mol Syst Biol.* **2**:2006.0008.
444 53. Huang JJ, Heiniger EK, McKinlay JB, Harwood CS. (2010) Production of hydrogen gas from light and the
445 inorganic electron donor thiosulfate by *Rhodopseudomonas palustris*. *Appl Environ Microbiol.*
446 **76**(23):7717–7722.
447 54. McKinlay JB, Zeikus JG, Vieille C. (2005) Insights into *Actinobacillus succinogenes* fermentative
448 metabolism in a chemically defined growth medium. *Appl Env Microbiol.* **71**(11):6651–6656.
449

Figure Legends

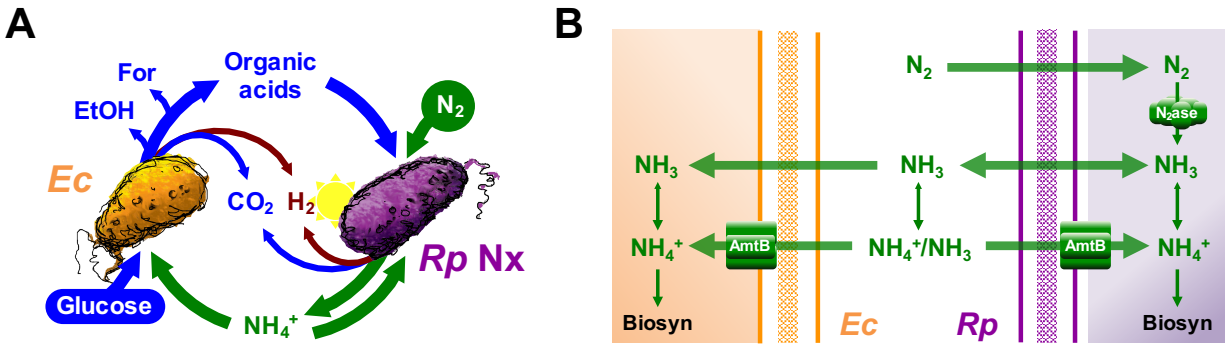

Fig. 1. Mechanisms of NH_4^+ transfer within an obligate bacterial mutualism based on cross-feeding of essential nutrients. (**A**) *Escherichia coli* (*Ec*) anaerobically ferments glucose into organic acids, supplying *Rhodopseudomonas palustris* Nx (*Rp* Nx) with essential carbon. *R. palustris* Nx fixes N_2 gas and excretes NH_4^+, supplying *E. coli* with essential nitrogen. For, formate; EtOH, ethanol. (**B**) NH_4^+ can be passively lost from cells as NH_3. Both species encode high-affinity NH_4^+ transporters, AmtB, that facilitate NH_4^+ uptake. NH_4^+ is the predominant form at neutral pH, as indicated by an enlarged arrow head on double-sided arrows.

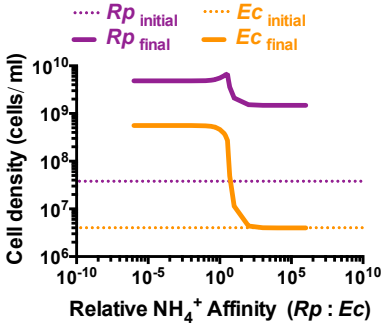

Fig. 2. Simulations suggest that *E. coli* must have a competitive advantage for NH_4^+ acquisition relative to *R. palustris* to support mutualistic growth. Final cell densities (solid lines) of *R. palustris* (*Rp*, purple) and *E. coli* (*Ec*, orange) after 300 h in simulated batch cultures for a range of relative NH_4^+ affinities. Initial cell densities are indicated by dotted lines. Relative NH_4^+ affinity values represent the relative *E. coli* K_m for NH_4^+ (K_A) divided by that of *R. palustris* (K_{AR}).

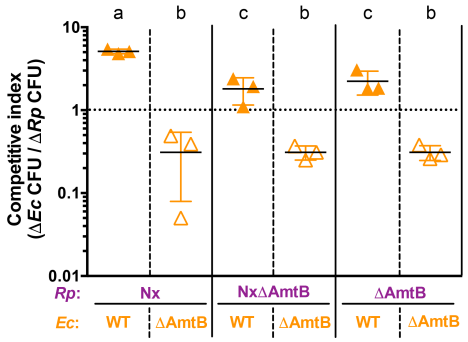

Fig. 3. AmtB is important for competitive NH_4^+ acquisition. Competitive indices for *E. coli* after 96 h in NH_4^+-limited competition assay cocultures. Cocultures were inoculated with *E. coli* and *R. palustris* at equivalent cell densities with excess carbon available for both species (25 mM glucose for *E. coli* and 20 mM sodium acetate for *R. palustris*). NH_4^+ was added to cocultures to a final concentration of 0.5 µM every hour for 96 h. The dotted line indicates a competitive index value of 1, where both species are equally competitive for NH_4^+. Filled triangles, WT *E. coli*; open triangles *E. coli* ΔAmtB. Error bars indicate SD, n=3. Different letters indicate statistical differences between *E. coli* competitive index values, $p < 0.05$, determined by one-way ANOVA with Tukey's multiple comparisons post test.

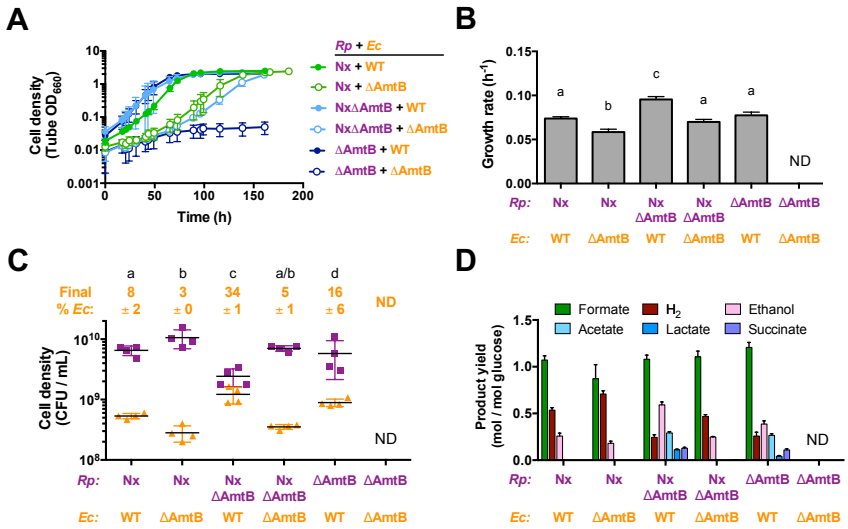

Fig. 4. NH_4^+ transporters influence population and metabolic trends of both partners in coculture. Growth curves (**A**), growth rates (**B**), final cell densities after one culturing (**C**), and fermentation product yields (**D**) from cocultures of all combinations of mutants lacking AmtB in each species. Final cell

densities and fermentation product yields were taken after one week, within 24 h into stationary phase. ND, not determined. Error bars indicate SD, n=4. Different letters indicate statistical differences, $p < 0.05$, determined by one-way ANOVA with Tukey's multiple comparisons post test.

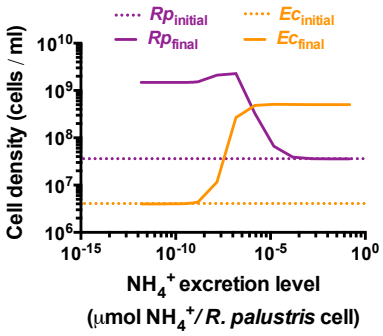

Fig. 5. Higher *R. palustris* NH_4^+ excretion levels are predicted to compensate for a low *E. coli* NH_4^+ affinity. 300 h batch cultures were simulated with a relative *R. palustris* : *E. coli* (*Ec* : *Rp*) K_m value for NH_4^+ of 0.001 over different *R. palustris* NH_4^+ excretion levels (R_A). Final cell densities, solid lines; initial cell densities, dotted lines.

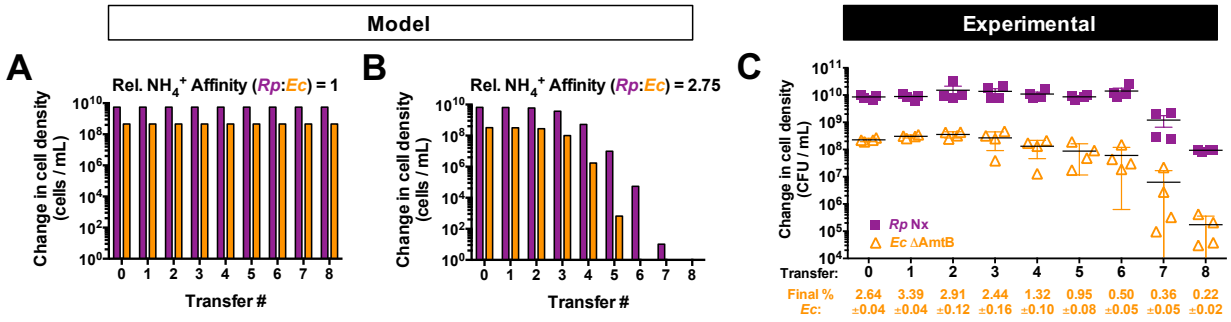

Fig. 6. A low *E. coli* NH_4^+ affinity results in coculture collapse over serial transfers when paired with *R. palustris* Nx. (**A**,**B**) 300 h batch cultures were simulated and serial transferred used a 1% inoculum based on the cell density at 300 h for the previous culture. Relative NH_4^+ affinity values represent the relative *E. coli* K_m for NH_4^+ (K_A) divided by that of *R. palustris* (K_{AR}). (**C**) Final cell densities of *R. palustris* Nx and *E. coli* ΔAmtB of cocultures grown for one week, less than 24 h into stationary phase. A 1% inoculum was used for each subsequent serial transfer. Error bars indicate SD, n=4. Final *E. coli* cell percentages +/- SD for each transfer are shown.

Recipient-biased competition for a cross-fed nutrient is required for coexistence of microbial mutualists

Alexandra L. McCully, Breah LaSarre, James B. McKinlay

Department of Biology, Indiana University, Bloomington

SI Appendix.

SyFFoN_v3 description.

Equations 1 – 4 were used to describe *E. coli* and *R. palustris* growth rates:

Eq. 1: *E. coli* growth rate; $\boldsymbol{\mu_{Ec}} = \mu_{EcMAX}\bullet[G/(K_G+G)]\bullet[A/(K_A+A)]\bullet[b_{Ec}/(b_{Ec}+10^{(f+C)})]$

Eq. 2: *R. palustris* growth rate (N_2); $\boldsymbol{\mu_{Rpn}} = \mu_{RpMAX}\bullet[C/(K_C+C)]\bullet[N/(K_N+N)]\bullet[b_{Rp}/(b_{Rp}+10^{(f+C)})]$

Eq. 3: *R. palustris* growth rate (NH_4^+); $\boldsymbol{\mu_{Rpa}} = \mu_{RpMAX2}\bullet[C/(K_C+C)]\bullet[A/(K_{AR}+A)]\bullet[b_{Rp}/(b_{Rp}+10^{(f+C)})]$

Eq 4: Total *R. palustris* growth rate; $\boldsymbol{\mu_{Rp}} = \mu_{Rpn} + \mu_{Rpa}$

Equations 5-14 were used to describe temporal changes in cell densities and extracellular compounds. Numerical constants in product excretion equations are used to account for molar stoichiometric conversions. Numerical constants used in sigmoidal functions are based on those values that resulted in simulations resembling empirical trends. All R and r parameters are expressed in terms of glucose consumed except for $R_{A,}$ which is the amount of NH_4^+ produced per *R. palustris* cell (Table S1).

Eq. 5: Glucose; $\boldsymbol{dG/dt} = -\mu_{Ec}\bullet Ec/Y_G - \mu_{Ec}\bullet Ec\bullet(R_c+R_f+R_e+R_{CO2}) - Ec\bullet(G/(K_G+G))\bullet(10/(10+1.09^{(1000\bullet\mu Ec)}))\bullet(b_{Ec}/(b_{Ec}+10^{(f+C)}))\bullet((100/(100+6^C))\bullet(r_C+r_f+r_e+r_{CO2}) + r_{C\_mono} + r_{f\_mono} + r_{e\_mono} + r_{CO2\_mono})$

Eq. 6: N_2; $\boldsymbol{dN/dt} = -\mu_{Rp}\bullet Rp\bullet 0.5\bullet Ra\bullet(1-(40/(40+1.29^N)) - \mu_{Rp}\bullet Rp/Y_N$

Eq. 7: Consumable organic acids; $\boldsymbol{dC/dt} = Ec\bullet\mu_{Ec}\bullet R_c\bullet 2 + Ec\bullet 2\bullet(G/(K_G+G))\bullet(10/(10+1.09^{(1000\bullet\mu Ec)}))\bullet(b_{Ec}/(b_{Ec}+10^{(f+C)}))\bullet(r_C\bullet(100/(100+6^C))+r_{C\_mono}) - (\mu_{Rp}\bullet Rp/Y_C) - 0.25\bullet Rp\bullet\mu_{Rp}\bullet Rh_{Rp} - 0.25\bullet Rp\bullet r_{Hp}\bullet(C/(K_C+C))\bullet(40/(40+1.29^N))\bullet(b_{Rp}/(b_{Rp}+10^{(f+C)}))$

Eq. 8: Formate; $\boldsymbol{df/dt} = (Ec\bullet\mu_{Ec}\bullet R_f\bullet 6) + Ec\bullet 6\bullet(G/(K_G+G))\bullet(10/(10+1.09^{(1000\bullet\mu Ec)}))\bullet(b_{Ec}/(b_{Ec}+10^{(f+C)}))\bullet(r_f\bullet(100/(100+6^C)) + r_{f\_mono}$

Eq. 9: NH_4^+; $\boldsymbol{dA/dt} = Rp\bullet\mu_{Rp}\bullet R_A\bullet(1-(40/(40+1.29^N))) - \mu_{Ec}\bullet Ec/Y_A - (\mu_{Rp}\bullet Rp/Y_{AR})\bullet(A/(K_{AR}+A))$

Eq. 10: *E. coli*; $\boldsymbol{dEc/dt} = \mu_{Ec}\bullet Ec$

Eq. 11: *R. palustris*; $\boldsymbol{dRp/dt} = \mu_{Rp}\bullet Rp$

Eq. 12: Ethanol; $\boldsymbol{de/dt} = Ec\bullet 3\bullet(\mu_{Ec}\bullet R_e + (G/(K_G+G))\bullet(10/(10+1.09^{(1000\bullet\mu Ec)}))\bullet(b_{Ec}/(b_{Ec}+10^{(f+C)}))\bullet(r_e\bullet(100/(100+6^C)) + r_{e\_mono}))$

Eq. 13: CO_2; $\boldsymbol{dCO2/dt} = Ec \bullet 6 \bullet (\mu_{Ec} \bullet R_{CO2} + (G/(K_G+G)) \bullet (10/(10+1.09^{(1000 \bullet \mu Ec)})) \bullet (b_{Ec}/(b_{Ec}+10^{(f+C)})) \bullet (r_{co2} \bullet (100/(100+6^{C})) + r_{co2\_mono})) + Rp \bullet 0.5 \bullet (\mu_{Rp} \bullet Rh_{Rp} + r_{Hp} \bullet (C/(K_C+C)) \bullet (40/(40+1.29^{N})) \bullet (b_{Rp}/(b_{Rp}+10^{(f+C)})))$

Eq. 14: H_2; $\boldsymbol{dH/dt} = Rp \bullet (\mu_{Rp} \bullet R_{HRp} + r_{Hp} \bullet (C/(K_C+C)) \bullet (40/(40+1.29^{N})) \bullet (b_{Rp}/(b_{Rp}+10^{(f+C)}))) + Ec \bullet (\mu_{Ec} \bullet R_{HEc} + (G/(K_G+G)) \bullet (10/(10+1.09^{(1000 \bullet \mu Ec)})) \bullet (b_{Ec}/(b_{Ec}+10^{(f+C)})) \bullet (r_H \bullet (100/(100+6^{C})) + r_{H\_mono}))$

Where,

μ is the specific growth rate of the indicated species (h^{-1}).

μ_{MAX} is the maximum specific growth rate of the indicated species (h^{-1}).

G, A, C, N, f, e, H and CO2 are the concentrations (mM) of glucose, NH_4^+, consumable organic acids, N_2, formate, ethanol, H_2, and CO_2, respectively. All gasses are assumed to be fully dissolved. Consumable organic acids are those that *R. palustris* can consume, namely, lactate (3 carbons), acetate (2 carbons), and succinate (4 carbons). All consumable organic acids were simulated to have three carbons for convenience. Only net accumulation of formate, ethanol, CO_2 and H_2 are described in accordance with observed trends.

K is the half saturation constant for the indicated substrate (mM).

Ec and Rp are the cell densities (cells/ml) of *E. coli* and *R. palustris*, respectively.

b is the ability of a species to resist the inhibiting effects of acid (mM).

Y is the *E. coli* or *R. palustris* cell yield from the indicated substrate (cells / µmol glucose). Y values were determined in MDC with the indicated substrate as the limiting nutrient.

R is the fraction of glucose converted into the indicated compound per *E. coli* cell during growth (µmol of glucose / *E. coli* cell), except for R_A. Values were adjusted to accurately simulate product yields measured in cocultures and in MDC with and without added NH_4Cl.

R_A is the ratio of NH_4^+ produced per *R. palustris* cell during growth (µmol / *R. palustris* cell). The default value was based on that which accurately simulated empirical trends.

r is the growth-independent rate of glucose converted into the indicated compound (µmol / cell / h). Default values are based on those which accurately simulated empirical trends in coculture.

$r_{\_mono}$ is the growth-independent rate of glucose converted into the indicated compound by *E. coli* when consumable organic acids accumulate. Default values are based on linear regression of products accumulated over time in nitrogen-free cell suspensions of *E. coli* (4).

Table S1. Default parameter values used in the model unless stated otherwise

Parameter	Value	Description (Units); Source
μ_{EcMAX}	0.2800	*E. coli* max growth rate (h^{-1}); Monoculture
μ_{RpMAX}	0.0772	*R. palustris* max growth rate (h^{-1}); Monoculture
μ_{RpMAX2}	0.0152	Boost on *R. palustris* growth rate in presence of NH_4^+ (h^{-1}); Monoculture[a]
G	25	Glucose (mM)
A	0.00005	NH_4^+ (mM); from initial $(NH_4)_6Mo_7O_{24}{\cdot}4H_2O$ concentration
C	0	Consumable organic acids (those that *R. palustris* was observed to consume: lactate, acetate, and succinate; mM)
N	70	N_2 (assumed to be fully dissolved; mM)
f	0	Formate (mM)
e	0	Ethanol (mM)
CO2	0	Carbon dioxide (mM)
K_G	0.02	*E. coli* affinity (Michaelis-Menten constant (K_m)) for glucose (mM); (1)
K_C	0.01	*R. palustris* affinity (K_m) for consumable organic acids (mM); Assumed
K_A	0.01	*E. coli* affinity for NH_4^+ (mM); (2)
K_{AR}	0.01	*R. palustris* affinity for NH_4^+ (mM); Assumed[b]
K_N	6	*R. palustris* affinity (K_m) for N_2 (mM)
Ec	0.4×10^7	*E. coli* cell density (cells / ml)
Rp	3.6×10^7	*R. palustris* cell density (cells / ml)
b_{Ec}	10^{43}	Resistance of *E. coli* to low pH (mM)
b_{Rp}	10^{32}	Resistance of *R. palustris* to low pH (mM)
Y_G	8×10^7	Glucose-limited *E. coli* growth yield (cells / µmol glucose); Glucose-limited *E. coli* culture
Y_A	1×10^9	NH_4^+-limited *E. coli* growth yield (cells / µmol NH_4^+); NH_4^+-limited *E. coli* culture
Y_C	2.5×10^8	Organic acid-limited *R. palustris* growth yield (cells / µmol organic acid); Acetate-limited *R. palustris* culture
Y_N	5×10^8	N_2-limited *R. palustris* growth yield cells / µmol N_2; N_2-limited *R. palustris* culture
R_C	1.9×10^{-8}	Fraction of glucose converted to organic acids (µmol glucose / cell)
R_f	8×10^{-9}	Fraction of glucose converted to formate (µmol glucose / cell)
R_e	4.5×10^{-9}	Fraction of glucose converted to ethanol (µmol glucose / cell)
R_{CO2}	5×10^{-10}	Fraction of glucose converted to CO_2 (µmol glucose / cell)
R_{HRp}	2×10^{-9}	*R. palustris* H_2 production (µmol H_2 / *R. palustris* cell)
R_{HEc}	5×10^{-9}	*E. coli* H_2 production (µmol H_2 / *E. coli* cell)
R_A	0.15×10^{-9}	*R. palustris* NH_4^+ production (µmol NH_4^+ / cell)
r_C	300×10^{-11}	*E. coli* specific growth-independent rate of glucose conversion to consumable organic acids (µmol glucose / cell / h) (3)
r_f	47×10^{-11}	*E. coli* specific growth-independent rate of glucose conversion to formate (µmol glucose / cell / h) (3)
r_e	15×10^{-11}	*E. coli* specific growth-independent rate of glucose conversion to ethanol (µmol glucose / cell / h) (3)
r_{CO2}	2×10^{-11}	*E. coli* specific growth-independent rate of glucose conversion to CO_2 (µmol glucose / cell / h) (3)

r_H	2×10^{-11}	*E. coli* specific growth-independent rate of H_2 production (µmol H_2 / cell / h) (3)
r_{C_mono}	1.2×10^{-11}	*E. coli* specific growth-independent rate of glucose conversion to consumable organic acids when consumable organic acids accumulate (µmol glucose / cell / h); (4)
r_{f_mono}	0.83×10^{-11}	*E. coli* specific growth-independent rate of glucose conversion to formate when consumable organic acids accumulate (µmol glucose / cell / h); (4)
r_{e_mono}	0.5×10^{-11}	*E. coli* specific growth-independent rate of glucose conversion to ethanol when consumable organic acids accumulate (µmol glucose / cell / h); (4)
r_{co2_mono}	1.3×10^{-11}	*E. coli* specific growth-independent rate of glucose conversion to CO_2 when consumable organic acids accumulate (µmol glucose / cell / h); (4)
r_{H_mono}	0.83×10^{-11}	*E. coli* specific growth-independent rate of glucose conversion to H_2 when consumable organic acids accumulate (µmol glucose / cell / h); (4)
r_{Hp}	27×10^{-11}	*R. palustris* specific growth-independent rate of H_2 production (µmol H_2 / cell / h)

[a] Increased growth rate in presence of NH_4^+ versus N_2 based on the difference in experimentally determined growth rates in *R. palustris* monocultures grown with either NH_4^+ or N_2 as a nitrogen source.

[b] K_{AR} was assumed to be equivalent to the published *E. coli* K_m (2) for NH_4^+ (K_A).

91 **Table S2. Strains, plasmids, and primers used in this study**

Strain or plasmid	**Description or Sequence (5'-3'); Designation**	**Source or Purpose**
***R. palustris* strains**		
CGA009	Wild-type strain; spontaneous Cm^R derivative of CGA001	(5)
CGA4004	CGA009 Δ*hupS* Δ*rpa2750*; Parent	(4)
CGA4005	CGA4004 *nifA**; Nx	(4)
CGA4021	CGA4005 Δ*amtB1* Δ*amtB2*; NxΔAmtB	(4)
CGA4026	CGA4004 Δ*amtB1* Δ*amtB2;* ΔAmtB	This study
***E. coli* strains**		
MG1655	Wild-type K12 strain, WT	(6)
K-12 JW0441-1	Keio collection Δ*amtB::Km*	(7)
MG1655ΔAmtB	MG1655 Δ*amtB::Km*; ΔAmtB	This study
Plasmids		
pJQnifA16	Gm^R; WT *nifA* gene flanked by XbaI/BamHI cloned into pJQ200SK	This study
Primers		
ALM6f	TTCGTCGCTGAATTGCAACG	*amtB* upstream flanking region (*E. coli*)
ALM6r	TCAGGAAGGGGTGATGCGTA	*amtB* downstream flanking region (*E. coli*)
JBM1	CGTCTAGACCGGCGCATCGC	*nifA16* upstream primer; XbaI
JBM6	GGGGATCCTGGTTCGCAGAGG	*nifA16* downstream primer; BamHI

92

SI Appendix Figures.

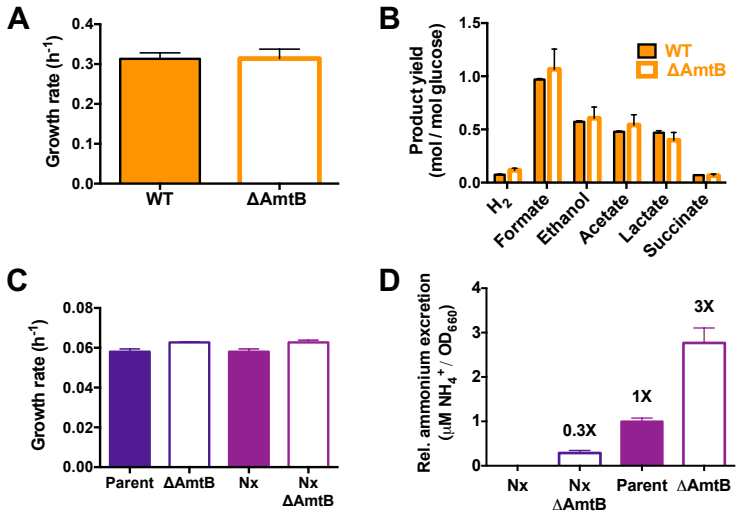

Fig. S1. ***E. coli*** **ΔAmtB and** ***R. palustris*** **ΔAmtB monoculture growth and metabolic trends.** (**A**,**B**) Growth rates (**A**) and fermentation product yields (**B**) from WT *E. coli* (filled) or without (open) *E. coli* ΔAmtB monocultures grown in MDC with 25 mM glucose and 15 mM NH_4Cl. Fermentation profiles were generated from stationary monocultures. Error bars indicate SD, n=3. (**C**,**D**) Growth curves (**C**) and relative NH_4^+ excretion (**D**) of *R. palustris* monocultures grown in MDC with 3 mM sodium acetate and a 100% N_2 headspace. Error bars indicate SD, n=4.

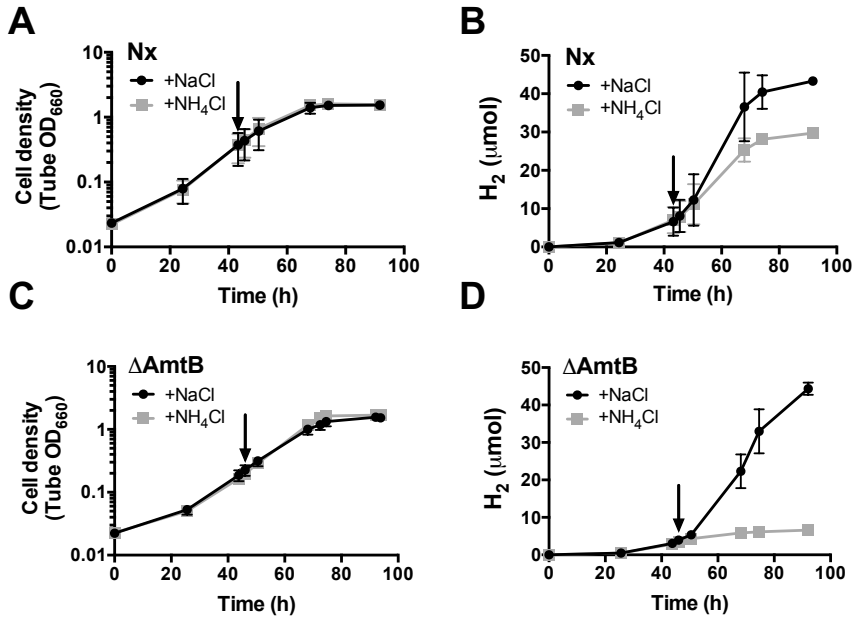

Fig. S2. *R. palustris* ΔAmtB responds to NH_4^+-induced shutoff of nitrogenase. The effect of either NH_4Cl or NaCl on growth (**A**,**C**) and H_2 production (**B**,**D**) in *R. palustris* Nx or *R. palustris* ΔAmtB monocultures. *R. palustris* monocultures were grown in MDC with 20 mM sodium acetate and a 100% N_2 headspace until mid-exponential phase and then supplemented with either 15 mM NH_4Cl or 15 mM NaCl at the time indicated by the arrow.

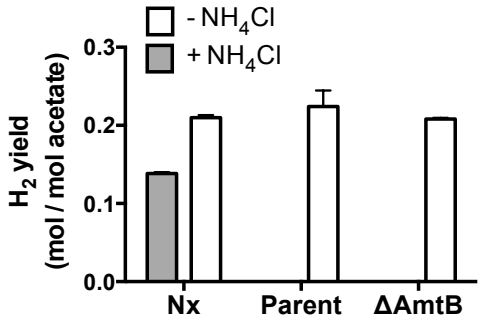

Fig. S3. Unlike *R. palustris* Nx, *R. palustris* ΔAmtB does not produce H_2 when grown with NH_4^+. *R. palustris* monocultures were grown in MDC with 20 mM sodium acetate and a 100% N_2 headspace with (grey) or without (white) 15mM NH_4Cl. Samples for determining H_2 yields were taken one week after inoculation, within 24 hours into stationary phase. Error bars indicate SD, n=3.

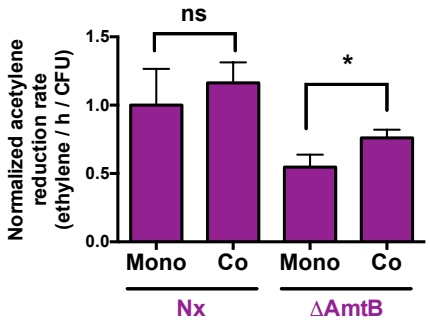

Fig. S4. *R. palustris* ΔAmtB nitrogenase activity increases in coculture. Normalized nitrogenase activity of *R. palustris* in monoculture (Mono) or coculture (Co) measured by an acetylene reduction assay. Ethylene levels were divided by total *R. palustris* CFUs in the test tube and then normalized to the *R. palustris* Nx monoculture value. Error bars indicate SD, n=4. *, statistical difference between monoculture and coculture conditions, $p < 0.05$, determined using multiple two-tailed t-tests; ns, no significant difference.

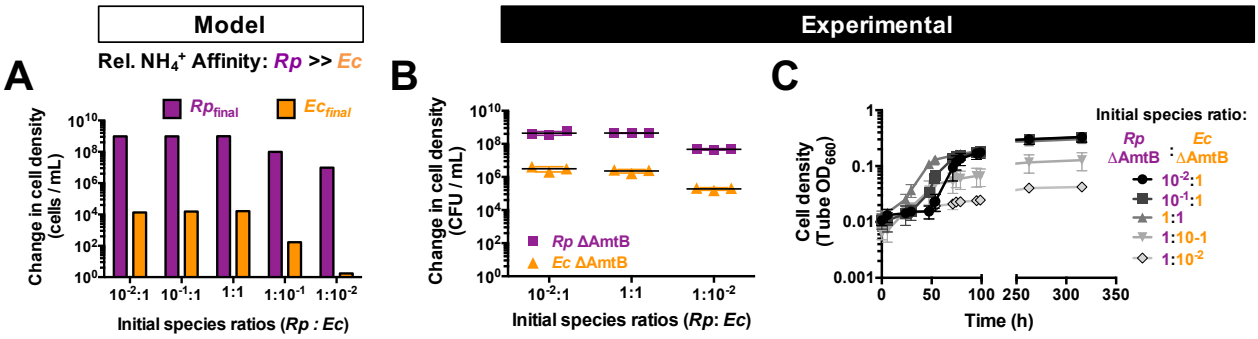

Fig. S5. Higher initial cell densities of *E. coli* ΔAmtB can partially compensate for a low *E. coli* NH_4^+ affinity. Simulations (**A**) and empirical data (**B**,**C**) showing the effect of initial *E. coli* (*Ec*) cell density on population and coculture growth trends when *E. coli* has a lower affinity for NH_4^+ compared to *R. palustris* (*Rp*). (**A**) 300 h batch cultures were simulated with a relative *R. palustris* : *E. coli* (*Rp* : *Ec*) K_m value for NH_4^+ of 0.001. (**B, C**) Change in cell densities after one week of growth (**B**) and growth curves (**C**) of cocultures inoculated at different species ratios. (**A-C**) A ratio value of 1 represents 2.7 x 10^6 CFUs/mL, which was experimentally measured from the starting inoculum for both species before diluting to achieve the indicated ratios. Error bars indicate SD, n=3.

SI Appendix References.

1. Buhr A, Daniels GA, Erni B. (1992) The glucose transporter of *Escherichia coli*: Mutants with impaired translocation activity that retain phosphorylation activity. *J Biol Chem.* **267**(6):3847–3851.

2. Khademi S, et al. (2004) Mechanism of ammonia transport by Amt/MEP/Rh: structure of AmtB at 1.35 A. *Science.* **305**(5690):1587–1594.

3. McCully AL, LaSarre B, McKinlay JB. (2017) Growth-independent cross-feeding modifies boundaries for coexistence in a bacterial mutualism. *biorXiv*. **doi:** https://doi.org/10.1101/083386

4. LaSarre B, McCully AL, Lennon JT, McKinlay JB. (2017) Microbial mutualism dynamics governed by dose-dependent toxicity of cross-fed nutrients. *ISME J*. **11**:337–348.

5. Larimer FW, et al. (2004) Complete genome sequence of the metabolically versatile photosynthetic bacterium *Rhodopseudomonas palustris*. *Nat Biotechnol.* **22**(1):55–61.

6. Hayashi K, et al. (2006) Highly accurate genome sequences of *Escherichia coli* K-12 strains MG1655 and W3110. *Mol Syst Biol.* **2**(1):2006.0007.

7. Baba T, et al. (2006) Construction of *Escherichia coli* K-12 in-frame, single-gene knockout mutants: the Keio collection. *Mol Syst Biol.* **2**:2006.0008.